

# Contribution of nucleoside-analogue reverse transcriptase inhibitor therapy to lipoatrophy from the population to the cellular level

David Nolan, Emma Hammond, Ian James, Elizabeth McKinnon and Simon Mallal\*

Centre for Clinical Immunology and Biomedical Statistics, Royal Perth Hospital and Murdoch University, Western Australia

\*Corresponding author: Tel: +61 8 9224 2899; Fax: +61 8 9224 2920; E-mail: S.Mallal@murdoch.edu.au

**Objectives:** It has been proposed that the contribution of nucleoside-analogue reverse transcriptase inhibitor (NRTI) therapy to subcutaneous fat wasting involves adipose tissue-specific mitochondrial DNA toxicity. We have investigated the relationships between NRTI therapy, adipocyte mitochondrial DNA content, evidence of toxicity in adipose tissue and fat wasting in Caucasian male Western Australian HIV Cohort study participants. **Methods:** Longitudinal mixed effects analysis of fat wasting was undertaken in individuals receiving initial stavudine- or zidovudine-containing highly active anti-retroviral therapy (HAART) ( $n=49$ , 149 DEXA measurements). Adipocyte mitochondrial DNA (mtDNA) depletion was also assessed according to current NRTI therapy in 92 subcutaneous fat biopsies from 69 HIV-positive individuals and seven healthy controls, and results were correlated with fat wasting among a subset of patients with biopsy data receiving initial stavudine- or zidovudine-containing HAART ( $n=22$ , 103 DEXA measurements). Confocal microscopy was performed in 22 biopsy samples obtained before and after initiating/switching NRTI therapy.

**Results:** Stavudine therapy was associated with more severe adipocyte mitochondrial DNA depletion ( $P<0.001$ ) and fat wasting over time ( $P=0.002$ ) compared with zidovudine therapy in independent analyses. Among patients with concurrent biopsy and longitudinal DEXA data, fat wasting was associated with duration of NRTI therapy ( $P=0.001$ ) and adipocyte mtDNA copies/cell ( $P=0.01$ ). In this analysis, the significant association between choice of stavudine versus zidovudine and fat wasting ( $P=0.03$ ) was lost after adjustment for the effect of mtDNA depletion ( $P=0.13$ ). Confocal analysis provided direct evidence of a relationship between severity of adipose tissue toxicity and mitochondrial DNA depletion. No significant effects of HIV protease inhibitor therapy were detected in these analyses.

**Conclusions:** Severity of subcutaneous fat wasting is primarily determined by choice of NRTI therapy (stavudine versus zidovudine) and by duration of exposure to the relevant NRTI. At the cellular level, evidence is provided that this effect manifests through NRTI-induced mitochondrial DNA depletion.

## Introduction

Antiretroviral therapy-associated lipodystrophy is characterized by pathological changes in body composition as well as lipid and glucose metabolism that occur in patients receiving long-term treatment for HIV infection. The dominant clinical feature within this syndrome is progressive loss of subcutaneous fat tissue over the limbs and face referred to as lipoatrophy or subcutaneous fat wasting [1,2]. Whilst the aetiology of fat wasting is incompletely understood, observational studies [3-5] as well as clinical trials [6-9] indicate that the choice of nucleoside-analogue reverse transcriptase inhibitor (NRTI) therapy significantly influences the risk of progression to clinically apparent subcutaneous fat wasting, and that NRTI therapy alone provides sufficient conditions for its development [9,10].

A mechanism linking NRTI therapy to subcutaneous fat wasting in which NRTI-induced

mitochondrial toxicity affecting adipose tissue is a key pathogenic factor has been proposed by Brinkman and colleagues [11], based on evidence that NRTI drugs selectively inhibit the human DNA polymerase responsible for mitochondrial DNA synthesis (polymerase- $\gamma$ ) independent of their capacity to inhibit HIV reverse transcriptase [12,13]. An approach to testing this hypothesis was also advanced, involving (1) prospective studies providing epidemiological evidence of the role of NRTI therapy in the development of the syndrome; (2) demonstration of mitochondrial dysfunction at the adipose tissue level; and (3) evidence linking the development of NRTI-induced mitochondrial toxicity to fat wasting. However, it was observed that the absence of a working case definition of the lipodystrophy syndrome limited the prospect of successfully establishing these causal links.

We have sought to examine the role of NRTI therapy in the pathogenesis of subcutaneous fat wasting comprehensively, according to the principles outlined by Brinkman and colleagues. A key element in these analyses is the conception of fat wasting as a continuous process of variable rate and severity, rather than as a dichotomous clinical outcome that is assigned as 'present' or 'not present'. In this way, the requirement for a case definition of lipodystrophy in this pathogenesis study is removed. These data provide convergent evidence that the choice of NRTI therapy (stavudine versus zidovudine) is the principal determinant of the severity of fat wasting over time, and that this NRTI-associated toxicity manifests specifically through adipocyte mitochondrial DNA depletion and adipose tissue toxicity.

## Materials and methods

### Clinical parameters

Clinical and laboratory data routinely collected in the Western Australian HIV Cohort Study and relevant to this study included age, race, weight, body mass index (BMI), presence of AIDS diagnosis, T cell subsets and history of antiretroviral drug use.

### *Longitudinal trends in subcutaneous leg fat*

Caucasian male participants in the Western Australian HIV Cohort Study were included in this analysis if they had a highly active antiretroviral therapy (HAART) regimen containing stavudine (d4T) or zidovudine (AZT) as their first antiretroviral therapy, and had undergone at least two dual energy X-ray absorptiometry (DEXA) scans during this initial HAART regimen. Measurements were not included after any change or interruption of treatment. Of the 49 patients satisfying these inclusion criteria, 25 received d4T [18 with lamivudine, seven with didanosine, 16 with protease inhibitor (PI) therapy] and 24 received AZT (24 with lamivudine, 18 with PI therapy). A total of 149 DEXA scans were considered. The maximum durations of initial HAART over which DEXA scans were recorded were similar in the two groups with the range for AZT 4.8–58.6 months (mean 31.4 months) and for d4T 5.5–53.1 months (mean 23.3 months), thus allowing estimation of models over comparable periods. AZT and d4T groups were well balanced (mean  $\pm$ SD) according to age (40.3  $\pm$ 10.7 vs 39.7  $\pm$ 9.6 years,  $P=0.8$ ), baseline CD4 T cell count (355  $\pm$ 189 vs 319  $\pm$ 178  $\times 10^9/l$ ,  $P=0.5$ ), and number of DEXA scans performed (3.1  $\pm$ 1.4 vs 3.0  $\pm$ 1.0). Pre-treatment BMI was slightly higher in the AZT group compared with the d4T group (25.3  $\pm$ 3.5 vs 23.3  $\pm$ 3.6 kg/m<sup>2</sup>,  $P=0.05$ ).

### *Subcutaneous fat biopsy study*

Ninety-two biopsies were obtained from 69 HIV-infected patients, and an additional seven biopsies were obtained from HIV-seronegative individuals. Tissue processing procedures were identical in these cases. All procedures, as well as storage and analysis of genetic material, were performed with informed consent from participants, and the study was approved by the Royal Perth Hospital ethics committee. In HIV-infected patients, biopsies were obtained from the supra-iliac region following a 5 cm surgical incision with direct dissection of adipose tissue, and samples were processed and immediately frozen in liquid nitrogen prior to storage at  $-70^\circ\text{C}$ .

Biopsy samples were classified into the following groups: (Group 1) HIV-seronegative controls ( $n=7$ , seven biopsies); (Group 2) antiretroviral therapy-naive HIV-infected individuals ( $n=23$ , 23 biopsies); (Group 3) individuals on current AZT therapy ( $n=28$ , 30 biopsies); (Group 4) individuals on current d4T therapy ( $n=24$ , 28 samples); and (Group 5) individuals receiving HAART regimens without d4T/AZT ( $n=10$ , 11 samples). All biopsies were analysed for adipocyte mitochondrial DNA content following collagenase digestion, and confocal microscopy was also undertaken in one HIV-seronegative control and in a subset of 10 patients (22 biopsies) with sequential biopsies obtained before and after initiating ( $n=7$ ) or switching ( $n=3$ ) NRTI therapy.

### Assessment of body composition

Body composition was assessed using a Hologic QDR-4500A DEXA scanner with enhanced array whole body software (version 8.23a:3). The primary endpoint used in the analysis of fat loss over time (%leg fat/BMI) reflects the regional distribution of subcutaneous fat (%leg fat derived from whole body DEXA scans) relative to a measure of generalized adiposity (BMI). In this way, assessment of the 'proportionality' of adipose tissue distribution allows adjustment for baseline (pre-treatment) differences in body composition, and particularly generalized adiposity, between individuals. The validity of this approach was assessed by determining the relationship of %leg fat to BMI in 40 white male subjects at baseline (that is, at the time of initiating antiretroviral therapy). A strong association between these two parameters was found ( $P<0.001$ ), with no significant departure from proportionality ( $P=0.23$ ) across a wide range of BMI values (mean  $\pm$ SD, 22.6  $\pm$ 3.0 kg/m<sup>2</sup>, range 17.3–30.1 kg/m<sup>2</sup>). Additionally, no differences were found between patients commencing AZT ( $n=21$ ) or d4T ( $n=19$ ) therapy ( $P=0.44$ ).

### Measurement of adipocyte mitochondrial DNA content

Tissues were incubated in 3% crude collagenase solution (Sigma) with 1.5% bovine serum albumin at 37°C for 80 min to digest stromal-vascular tissue. Total DNA was extracted using QIAamp DNA MIDI Kit (Qiagen, Inc., Chatsworth, Calif., USA) according to the manufacturer's tissue DNA extraction protocol. Mitochondrial and nuclear DNA copy numbers were measured by real-time PCR, using Taqman chemistry on the 7700 sequence detection system platform (Perkin-Elmer Applied Biosystems, Inc.) as previously described [19]. This assay has been validated in an international quality assurance study [14].

### Confocal microscopy

Immunohistochemical staining was performed on frozen biopsy material for the purposes of detecting morphological evidence of cellular toxicity. Specifically, to detect whether reduced mtDNA content (as detected using the quantitative PCR assay) resulted in reduced expression of mtDNA-encoded protein subunits compared with nDNA-encoded subunits, we fluorescently labelled subunit I (mtDNA-encoded) and subunit IV (nDNA-encoded) of cytochrome c oxidase – the fourth protein complex in the mitochondrial respiratory chain. A nuclear DNA stain was included as a counterstain for cell orientation. Tissue sections (<1 mg) were incubated in a solution of anti-COX IV primary antibody (5 µg/ml) at 4°C for 4.5 h. Tissues were washed for 3 h in phosphate buffered saline (PBS) with 1% bovine serum albumin (BSA) at 4°C, and incubated overnight at 4°C in a solution of secondary antibody (5 µg/ml) labelled with fluorophore AF546, 0.4 µm Hoechst 33342 and 0.5 µg/ml of an anti-COX I antibody that was directly conjugated with fluorophore AF488. All reagents were obtained from Molecular Probes, Eugene, Oreg., USA. Tissues were washed with 1 ml of PBS plus 1% tween 20 for 3 h, before being mounted with 90% glycerol in concave glass slides.

Separate staining to detect macrophages was performed using either primary mouse monoclonal antibodies MAC 387 (215 ng/ml) or CD68 (380 ng/ml) (DAKO, Glustrop, Denmark), and a secondary anti-mouse antibody labelled with fluorophore AF546 (5 µg/ml), together with a Hoechst 33342 counterstain.

A fluorescent microscope equipped with a Bio-Rad MRC 1024 UV confocal laser scanning system, controlled by Laserssharp image acquisition, was used to capture digital images of stained tissue. Visualization of fluorophore AF488 was achieved by laser excitation at a 488 nm line from an argon laser and emissions were detected through a 522/35 nm bandpass filter. Visualization of fluorophore AF546 was achieved by

laser excitation at a 543 nm line from a green Helium Neon laser and emissions were detected through a 580/32 nm band passfilter. Hoechst staining of nuclear DNA was visualized by excitation using the 351 nm line from an argon UV laser and detection was through a 455/30 nm band pass filter. All images for longitudinal samples were acquired during the same day for all experimental conditions, using identical instrument settings that avoided saturation of the brightest pixels. An average of 16 sequential tissue images was collected separately by Kalman, averaging 3 frames/image for each separate fluorophore using a Nikon 40X, NA 1.3 oil immersion objective at optical zoom of 1, 1.5 or 2. The series of optical sections was collected at 0.5–2 µm increments along a z-axis. Confocal assistant software was used to merge the three fluorophore data files into one for each scan and then to compile 3-dimensional rotational views of sequential scans. The red (COX IV subunit) and green (COX I subunit) fluorophores, co-localizing as yellow to identify the COX multiprotein were assessed using Laserssharp 3.1 software and showed a co-localization coefficient of 95%. Shifts from baseline in the yellow colour of co-localized COX subunits to a red spectrum were interpreted as a reduction in the ratio of COX-I (green) to COX-IV (red) subunit expression. Images were reviewed independently by a histopathologist blinded to the clinical status and treatment history of the subjects.

### Statistical analysis

Statistical analysis utilized the S-PLUS statistical package (S-PLUS 6 for Windows, Insightful Corporation, Seattle, Wash., USA). Analyses of longitudinal trends in leg fat and of adipocyte mitochondrial DNA copies/cell were based on mixed effects analysis, allowing adjustment for effects of multiple measurements on individuals. Statistical significance of effects was determined using standard Wald tests.

The study of longitudinal trends in leg fat utilized a non-linear mixed effects model of the form:

$$\% \text{leg fat/BMI} = r_0 - d * (1 - \exp(-k * \text{time}))$$

with  $k > 0$  and *time* equal to the time (months) from commencement of HAART. In this model  $r_0$  represents the baseline value, and  $d$  the difference between baseline and the value approached by the %leg fat/BMI ratio as time becomes large (the asymptote). The rate of decline of leg fat over time from the commencement of HAART depends on both  $d$  and the moderating parameter  $k$ . Each of the parameters ( $r_0$ ,  $d$  and  $k$ ) may depend on the covariates under consideration and in addition the mixed effects model allows individual variation (random effects) in the profiles.

## Results

### Longitudinal trends in subcutaneous leg fat

Initial analysis was restricted to 49 white males who were antiretroviral therapy-naive prior to commencing HAART (DEXA scans=149). Although baseline BMI was lower in the d4T group, no significant difference in %leg fat/BMI ratios at commencement of HAART between these groups was detected (average 0.98,  $P>0.5$ ).

BMI was not significantly influenced over time by use of HAART in either the AZT or d4T treatment groups ( $P=0.3$ ). However, average %leg fat/BMI decreased exponentially in both groups, with a significantly greater decline for those patients receiving d4T than for those receiving AZT ( $P=0.002$ , Table 1), before levelling off after approximately 36 months of HAART (Figure 1). At 36 months, average %leg fat

decreased by 56% in patients receiving d4T and by 31% in those receiving AZT.

No significant effects were found of baseline CD4 T cell count or of PI use or didanosine use on the average profiles of %leg fat/BMI ( $P>0.2$ ). Excluding didanosine therapy to restrict the dataset to d4T/lamivudine and AZT/lamivudine recipients only ( $n=42$ , DEXA scans=128) produced similar results (d4T vs AZT,  $P=0.006$ , Table 1). Patients younger than 35 years had lower average initial ratios of %leg fat to BMI (average 0.85,  $P=0.04$ ) but had a smaller decrease over time ( $P=0.01$ ) leading to 'flatter' profiles, with lower %leg fat/BMI ratios at baseline and higher long-term levels. We found no significant difference between profiles for those aged 35–45 or greater than 45 ( $P=0.4$ ).

**Table 1.** Parameter estimates for population average profiles of %leg fat relative to BMI following commencement of initial HAART

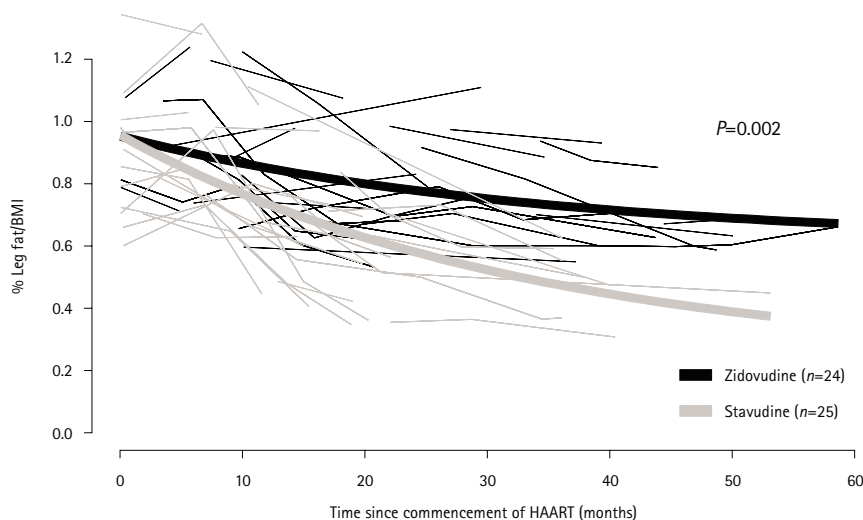
Parameter		Initial HAART		
		Estimate	SE	P-value
$r_0$	Constant	1.005	0.040	
	Age <35	-0.140	0.061	0.025
$d$	Constant	0.471	0.102	
	Age <35	-0.337	0.116	0.005
	d4T use*	0.389	0.124	0.002
$\log(k)$		-3.524	0.349	

\*Excluding didanosine recipients; estimated effect of d4T use =0.33; SE=0.18;  $P=0.006$ .

### Adipocyte mitochondrial DNA content

Comparisons of adipocyte mitochondrial DNA copies/cell according to current NRTI treatment are presented in Table 2 and Figure 2. Adipocyte mitochondrial DNA content was similar in the HIV-infected control group ( $n=23$ , median 1335 copies/cell), HIV-negative controls ( $n=7$ , median 1738 copies/cell), and in those receiving regimens excluding AZT/d4T ( $n=10$ , median 1522 copies/cell) ( $P>0.5$ ). In the AZT group ( $n=28$ , median 750 copies/cell), mitochondrial DNA content was significantly reduced compared with HIV-infected controls ( $P=0.006$ ). Mitochondrial DNA content was significantly reduced in the d4T group ( $n=24$ , 246 copies/cell), compared with both HIV-infected controls and AZT-treated individuals ( $P<0.001$ ). Utilizing the HIV-infected control group median value as a reference, median adipocyte mtDNA content was reduced to 18% of this value in

**Figure 1.** Longitudinal leg fat profiles for males on initial HAART receiving zidovudine and stavudine, and estimated average profiles for groups



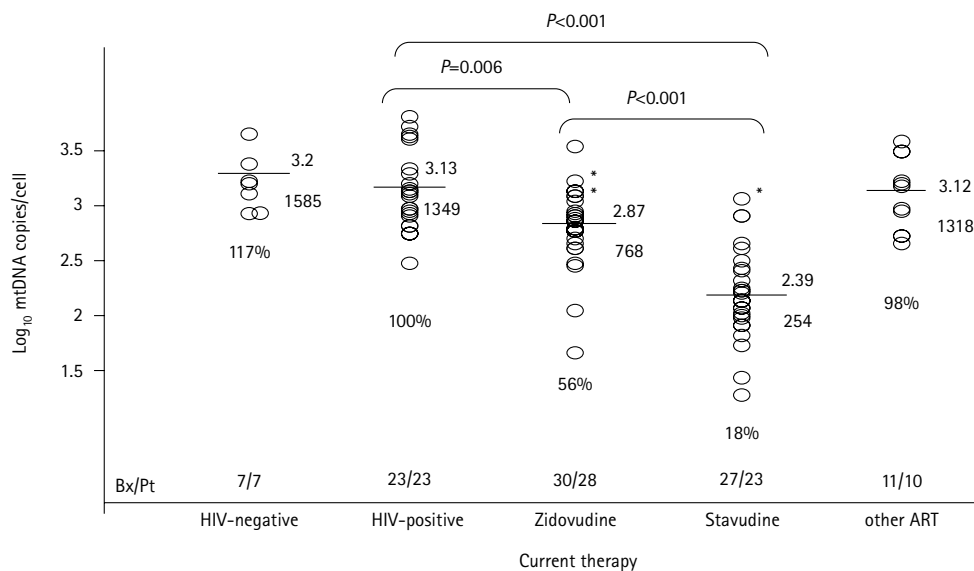
Average values for covariates utilized for estimated trends.

**Table 2.** Subcutaneous fat biopsy study: clinical parameters and mitochondrial DNA copies/cell in HIV-infected groups

Variable	HIV-infected controls	Zidovudine	Stavudine	P-values ( <sup>†</sup> AZT vs d4T)
Number of biopsy samples	23	30	28	
Number of patients	23	28	24	
Current lamivudine therapy		97%	82%	
Current PI therapy		47%	36%	
Age	45.3 ±10.2	45.3 ±10.3	46.3 ±9.6	0.9
CD4 count at time of biopsy	337 ±402	591 ±286	606 ±235	<0.006 ( <sup>†</sup> 0.83)
Current NRTI (months)		28.6 ±23.4	26.1 ±19.4	0.66
Mean log <sub>10</sub> mtDNA copies/cell (95% confidence intervals)	3.13 (3.00–3.25)	2.87 (2.75–3.00)	2.39 (2.27–2.51)	<0.001 ( <sup>†</sup> 0.001)
Median mtDNA copies/cell* (95% confidence intervals)	1335 (993–1797)	750 (557–1009)	246 (185–327)	
mtDNA depletion (% of control) (95% confidence intervals)	'100%'	56.1% (41.7–75.5)	18.4% (13.9–24.5)	

\*The mtDNA copies/cell values presented here are derived directly from the log<sub>10</sub> mtDNA copies/cell values for ease of interpretation and estimate the median values of the non-logged data.

**Figure 2.** Comparisons of adipocyte mitochondrial DNA copies/cell according to current NRTI therapy (see Table 2)



\*<6 weeks therapy; n=76 patients, 99 biopsies.

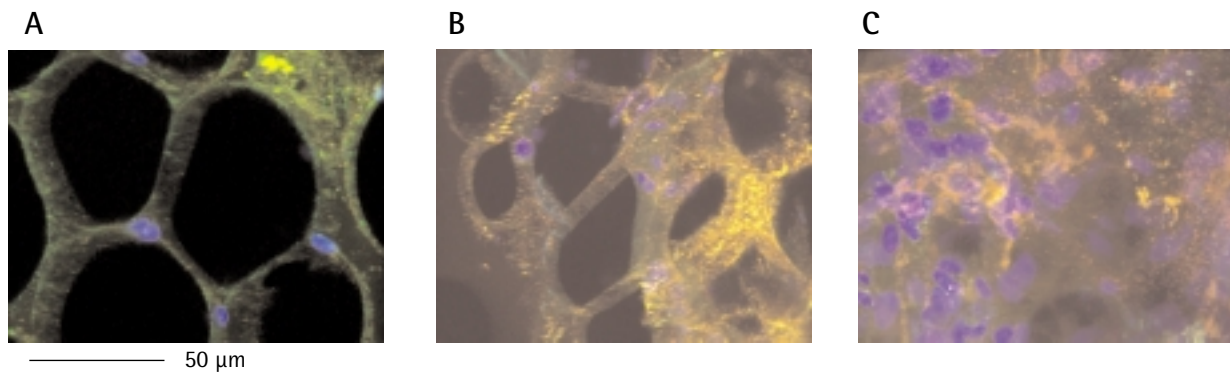
the d4T-treated group, and to 56% in those treated with AZT therapy (Table 2). Significant differences between d4T/lamivudine (n=23) and AZT/lamivudine (n=29) regimens were also found (P=0.002).

Commencing/switching NRTI therapy was associated with significant changes in mtDNA levels within 2–12 months in sequential biopsy samples (n=20, 40 biopsies, P<0.001). For patients initiating therapy (AZT=4, d4T=5), mtDNA levels decreased significantly from baseline (P=0.001), while switching from d4T therapy (n=6) resulted in significant increases in adipocyte mtDNA copies/cell (P=0.008). No association between mtDNA levels and use of HIV PIs was detected (P=0.8), and CD4 T cell counts at the time of

biopsy were also similar between NRTI treatment groups (P=0.8).

#### Relationship between %leg fat/BMI and adipocyte mitochondrial DNA content

Associations between %leg fat/BMI and mitochondrial DNA (mtDNA) depletion during initial AZT- or d4T-based HAART were also investigated via linear mixed models in a subset of patients with longitudinal DEXA data and fat biopsy data who had only received either d4T- (n=9) or AZT-containing therapy (n=13), including 103 DEXA scans in total. In this analysis, the rate of decline in %leg fat/BMI ratio was associated with duration of NRTI therapy (P=0.001) and severity

**Figure 3.** Confocal images of sequential biopsies prior to and after initiating antiretroviral therapy

(A) Antiretroviral therapy-naïve (leg fat=19%). Fine membrane structure of adipocytes, large non-staining lipid droplet, and small numbers of blue staining nuclei. Mitochondrial COX protein is labelled by green (COX subunit I) and red (COX subunit IV) fluorophores that co-localize as yellow.  
 (B) 7 months stavudine (leg fat=20%). Compared with (A), adipocytes are less spherical in shape and smaller in volume, with increased intercellular space. Fluorescent staining shows patches of intense yellow-labelled COX, indicating up-regulated mitochondrial protein expression. A shift from yellow to orange fluorescence indicates relative depletion of green-labelled COX subunit I.  
 (C) 13 months stavudine (leg fat=10%). Compared with (A), adipocytes are less frequent and markedly smaller, with increased intercellular space. Staining shows a marked shift from yellow to red fluorescence, indicating relative depletion of green-labelled COX subunit I. Nuclei are more frequent and large in size (15 μm), consistent with macrophage morphology.

of adipocyte mitochondrial DNA depletion ( $P=0.01$ ). After adjusting for adipocyte mtDNA copies/cell there was no significant difference in the rate of decline between AZT and d4T use ( $P=0.13$ ), while this difference was significant without adjustment ( $P=0.03$ ). Inclusion of a AZT/d4T effect did not abrogate the adipocyte mtDNA effect ( $P=0.03$ ), as would be expected if the effect of NRTI therapy on fat wasting manifests through differential effects on mtDNA depletion.

#### Confocal analysis of adipose tissue biopsies

Confocal imaging of antiretroviral-naïve samples (seven HIV-infected, one HIV-seronegative) demonstrated moderate numbers of spherical adipocytes with small nuclei within a delicate reticular tissue architecture. Mitochondrial cytochrome c oxidase (COX) protein was detected in the cytoplasm surrounding non-staining lipid droplets, most strongly in the perinuclear region (Figure 3a). By comparison, samples obtained after commencing NRTI therapy in the seven HIV-infected patients revealed evidence of tissue toxicity characterized by pleiomorphic adipocytes with reduced lipid droplet volume, increasing intercellular space, and increasing numbers of large (non-adipocyte) nuclei including prominent CD68- and MAC387-positive macrophages. Increased severity of mtDNA depletion paralleled the severity of adipose tissue toxicity in these samples (Figures 3b and 3c).

Sequential biopsies were obtained before and after switching from d4T to AZT therapy in three patients who changed therapy in an attempt to reverse clinically overt fat wasting (Table 3). In these samples, mtDNA depletion and characteristic adipose tissue toxicity were observed in the initial biopsy. After 5–12 months of switching from d4T to AZT, marked increases in

mitochondrial DNA copies/cell were observed (increasing 312–1202% from baseline). These increases were accompanied by detectable improvement in tissue toxicity in one of three cases, characterized by reductions in adipocyte pleiomorphism and intercellular space (Table 3).

In five of seven biopsies with marked mtDNA depletion (<300 copies/cell), there was a substantial shift in COX staining from yellow to red, signifying reduced expression of the mitochondrial DNA-encoded subunit I relative to nuclear DNA-encoded subunit IV. Tabulation of results for all confocal microscopy samples is provided in Table 3.

#### Discussion

These data provide multiple lines of evidence that adipose tissue mitochondrial toxicity associated with NRTI therapy has a prominent role in the pathogenesis of subcutaneous fat wasting. The analysis of fat wasting as a continuous process also reveals that subtle alterations in body composition, which may be insufficiently severe to be diagnosed as ‘lipodystrophic’, occur in patients treated with AZT or d4T. Hence, the severity of fat wasting, including cases where the pathological process is sub-clinical, is a product of the choice of NRTI (d4T vs AZT), as well as the duration of exposure to the relevant NRTI.

In both AZT and d4T treatment groups average trends in leg fat followed an exponential trajectory with a gradual deceleration of the rate of fat loss and a tendency to level off after approximately 3 years of therapy. This is in keeping with a plateau effect observed previously [15]. The dominant effect of NRTI therapy in determining the rate and severity of fat

**Table 3.** Confocal analyses of longitudinal fat biopsies prior to and after initiating/switching NRTIs

Patient case number	Time on current therapy	Fat wasting	mDNA copies/cell <sup>§</sup>	mDNA copies/cell (% decrease from baseline)	COX relative decrease subunit I/IV	Immunofluorescent staining and detection with confocal microscopy			
						Nuclei detected	Adipocyte shape	Intercellular space	Other anomalies
1	Healthy control	No wasting	1028	ND	ND	Normal	Regular	Normal	
<i>Patients who initiated therapy</i>									
36	ART-naive	24% leg fat	1040	ND	ND	Normal	Regular	Normal	
36	6 months d4T/3TC/rit/lop	26% leg fat	276	74	Detected	Markedly increased	Pleiomorphic	Increased	Fibres/increased macrophages
15	ART-naive	22% leg fat	761	ND	ND	Normal	Regular	Normal	
15	7 months d4T/3TC/rit/lop	24% leg fat	198	74	Detected	Markedly increased	Pleiomorphic	Increased	Fibres/adipocyte loss
18	ART-naive	20% leg fat	691	ND	ND	Normal	Regular	Normal	Increased macrophages
18	7 months d4T/3TC/ABC	19% leg fat	258	63	Detected	Normal	Smaller, pleiomorphic	Increased	Fibres
18	13 months d4T/3TC/ABC	10% leg fat	149	78	Marked	Markedly increased	Markedly smaller	Markedly increased	Adipocyte cell loss
22	ART-naive	21% leg fat	670	ND	ND	Normal	Regular	Normal	
22	8 months d4T/3TC/rit	25% leg fat	579	14	ND	Increased	Regular	Normal	
24	ART-naive	35% leg fat	3606	ND	ND	Normal	Regular	Normal	
24	8 months AZT/3TC/rit	42% leg fat	695	81	ND	Normal	Smaller, pleiomorphic	Increased	
12	ART-naive	BMI=21*	3388	ND	ND	Normal	Smaller	Normal	
12	6 months AZT/3TC/rit	BMI=30	832	75	ND	Normal	Normal	Normal	
11	ART-naive	28% leg fat	3320	ND	ND	Normal	Regular	Normal	
11	6 months AZT/3TC/efav	29% leg fat	751	77	ND	Normal	Regular	Normal	Fibres
<i>Patients who switched therapy</i>									
17	15 months d4T/ddI/ABC	11% leg fat	219	Detected	Detected	Markedly increased	Pleiomorphic	Increased	
17	5 months AZT/3TC/ABC	12% leg fat	2846	-1202	ND	Slightly increased	Normal	Normal	
29	20 months d4T/3TC/nel	14% leg fat	173	ND	ND	Slightly increased	Very pleiomorphic	Moderately increased	
29	12 months AZT/3TC/ABC	13% leg fat	713	-312	ND	Slightly increased	Pleiomorphic	Increased	
9*	39 months d4T/3TC/ddI	7% leg fat	213	ND	ND	Slightly increased	Pleiomorphic, elongated	Markedly increased	Multi-loculated adipocytes
9*	24 months AZT/3TC/ABC	8%	1089	-411	ND	Slightly increased	Pleiomorphic, elongated	Markedly increased	Multi-loculated adipocytes
9*	8 months AZT/3TC/ABC	7% leg fat	981	-360	ND	Slightly increased	Pleiomorphic, elongated	Increased	Multi-loculated adipocytes

ART, antiretroviral therapy; d4T, stavudine; 3TC, lamivudine; ABC, abacavir; lop, lopinavir; efav, efavirenz; rit, ritonavir; AZT, zidovudine; ddI, didanosine; BMI, body mass index; ND, not detected. \*AIDS-associated wasting; †Buffalo hump; § as measured by quantitative PCR.

wasting is also consistent with clinical trials comparing these NRTI drugs in both the presence and absence of HIV PI therapy [6–9], in which the incidence of clinically overt fat wasting was ~40–50% of d4T recipients compared with ~10–20% of AZT-treated patients over a 30 month period [6–8]. Furthermore, d4T substitution has been associated with statistically significant improvement in fat wasting compared with ongoing d4T treatment [16] – a finding that has not been observed in over 30 studies investigating the effects of switching HIV PI therapy [17]. However, reversal of fat wasting appears to be a slow and potentially incomplete process [16], so that avoidance of fat wasting appears to be more prudent than attempting to reverse the pathological process once it is established.

These data also support the hypothesis that NRTI therapy-associated adipose tissue mitochondrial toxicity is a key factor in the pathogenesis of fat wasting. First, highly significant differences in adipocyte mitochondrial DNA content were noted according to use of AZT or d4T therapy, consistent with the severity of fat wasting associated with these drugs. These effects occurred early in the course of NRTI therapy, suggesting that the severity of NRTI-induced adipocyte mitochondrial DNA depletion may be a critical early determinant of adipose tissue pathology and fat wasting. These findings are consistent with data from another Australian cohort study involving 62 subjects who underwent sequential fat biopsies at 6-monthly intervals (160 biopsies, average 2.6/patient). In this study, mitochondrial DNA depletion measured by real-time PCR was associated with choice of NRTI therapy (d4T vs AZT,  $P=0.001$ ) but was not influenced by duration of NRTI therapy ( $P=0.9$ ) in a similar mixed effects analysis [18].

Secondly, the severity of adipocyte mitochondrial DNA depletion and the duration of this effect (time on NRTI therapy), were found to be significantly associated with subcutaneous fat loss in a subset of patients with longitudinal DEXA scan data and fat biopsy data. Choice of NRTI therapy had no significant impact on leg fat wasting after adjustment for the effect of mitochondrial DNA depletion in this analysis, suggesting that the effect of NRTI therapy on fat wasting manifests specifically through mitochondrial DNA depletion in adipose tissue.

Finally, confocal analysis of adipose tissue from patients with sequential biopsy samples demonstrates adipose tissue toxicity, occurring early in the course of NRTI therapy, which was consistently related to the severity of mitochondrial DNA depletion. Adipose tissue changes observed with confocal microscopy are in keeping with distinct adipose tissue histopathological abnormalities previously observed,

characterized by adipocyte cell loss, formation of macrophage-laden lipogranulomata and increased tissue vascularity [19], as well as ultrastructural changes including cytoplasmic expansion and abnormal mitochondrial morphology [19–21]. Adipocyte apoptosis has also been observed *in vivo*, with evidence for improvement following d4T discontinuation associated with increased adipose tissue mitochondrial DNA content [22], but no change after discontinuing PI therapy while maintaining NRTI therapy [23].

A proposed pathogenic model of subcutaneous fat wasting, emphasizing the process as one of variable severity both at the cellular and clinical levels, is provided in Figure 4. Our data indicate that NRTI-induced mitochondrial DNA depletion and cellular toxicity occur fairly rapidly; eventually causing sufficient adipose tissue pathology to be discerned as lipoatrophy.

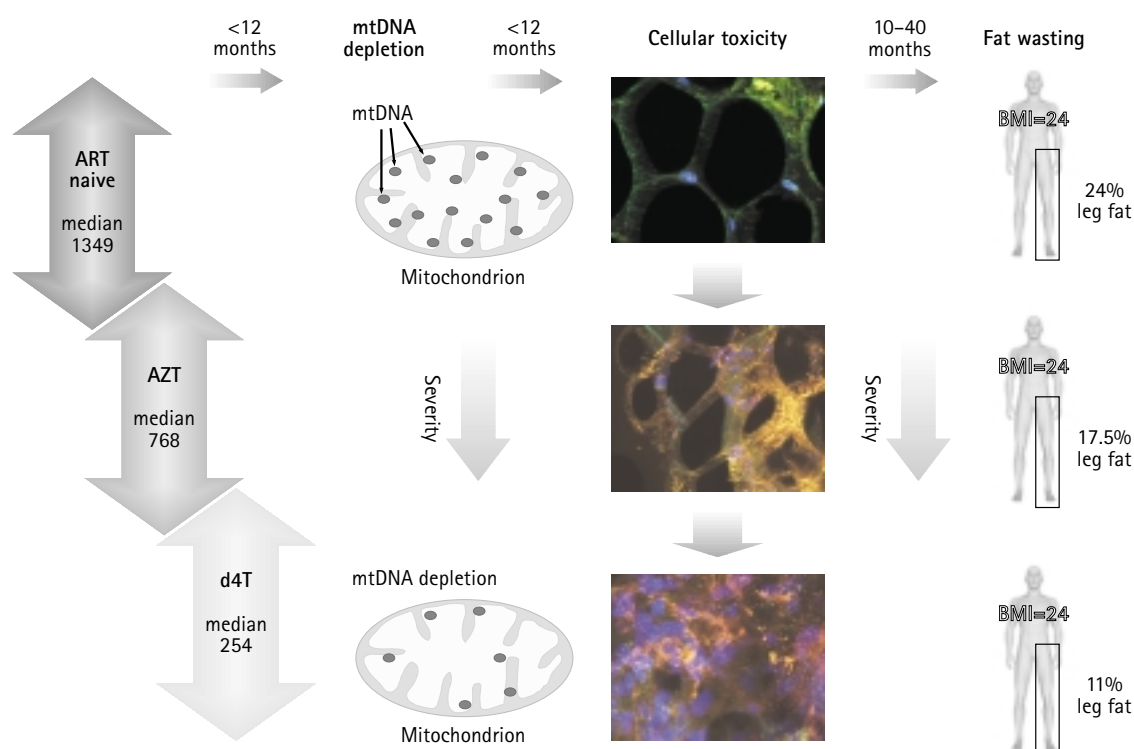
In relation to the role of PI therapy in lipodystrophy pathogenesis, these and other data [3,9] including the results of switching studies [17], suggest that the effect of PI therapy on peripheral fat wasting is relatively minor. However, given that the ‘lipodystrophy syndrome’ may be defined by the presence of fat accumulation and/or metabolic abnormalities, in addition to the presence of peripheral fat wasting [1,2], it is also likely that PI therapy contributes significantly to this composite definition. Certainly, there is now strong evidence that use of PI therapy is strongly associated with insulin resistance and dyslipidaemia [24–29], consistent with a ‘metabolic syndrome’ phenotype [30], and that withdrawing PI therapy improves these metabolic complications [16].

In conclusion, NRTI treatment, and d4T in particular, results in mitochondrial DNA depletion in adipocytes and adipose tissue toxicity which manifests as a process of pathological subcutaneous fat loss relative to total body mass. The progression of fat wasting represents a product of the severity of adipocyte mitochondrial DNA depletion, determined relatively early in the course of d4T or AZT treatment, and the period over which this effect is maintained. These findings provide a rational basis for the prevention of fat wasting among patients receiving long-term antiretroviral therapy.

### Conflict of interest statements

Simon Mallal, David Nolan, Ian James and Elizabeth McKinnon have spoken at meetings sponsored by GlaxoSmithKline, and Simon Mallal has sat on the advisory boards of GlaxoSmithKline, Bristol-Myers Squibb, and Merck Sharpe and Dohme.

Figure 4. Model of subcutaneous fat wasting pathogenesis



## Author contributions

David Nolan designed and implemented the subcutaneous fat biopsy study, performed adipose tissue biopsies, designed and wrote the manuscript, and contributed to statistical analysis.

Emma Hammond performed PCR-based quantitation of adipocyte mitochondrial DNA content, confocal microscopy and contributed to manuscript preparation.

Ian James and Elizabeth McKinnon designed and carried out the statistical analyses, and contributed to manuscript preparation.

Simon Mallal oversaw the conception and design of the studies, and contributed to the manuscript preparation.

David Nolan and Emma Hammond contributed equally to this work.

## Acknowledgements

We are grateful to the participants in the Western Australian HIV Cohort Study for their involvement in this research, to Cecily Metcalf for independently validating tabulation of the tissue morphology and to Craig Pace for processing adipose tissue samples. Confocal microscopy images were collected at the

Biomedical Confocal Microscopy Research Centre, sponsored by the Lotteries Commission of Western Australia, with the assistance of Paul Rigby. The invaluable intellectual input of Jean Himms-Hagen in the early stages of this research is also gratefully acknowledged.

This research was funded by NHMRC grant #194808, and an unrestricted educational grant from GlaxoSmithKline. These funding sources had no role in study design or manuscript preparation.

## References

1. Carr A, Samaras K, Thorisdottir A, Kaufmann GR, Chisholm DJ & Cooper DA. Diagnosis, prediction, and natural course of HIV-1 protease-inhibitor-associated lipodystrophy, hyperlipidaemia, and diabetes mellitus: a cohort study. *Lancet* 1999; 353:2093–2099.
2. John M, Nolan D & Mallal S. Antiretroviral therapy and the lipodystrophy syndrome. *Antiviral Therapy* 2001; 6:9–20.
3. Bernasconi E, Boubaker K, Junghans C, Flepp M, Furrer HJ, Haensel A, Hirschel B, Boggian K, Chave JP, Opravil M, Weber R, Rickenbach M & Telenti A; Swiss HIV Cohort Study. Abnormalities of body fat distribution in HIV-infected persons treated with antiretroviral drugs: the Swiss HIV Cohort Study. *Journal of Acquired Immune Deficiency Syndromes* 2002; 31:50–55.
4. Mallal SA, John M, Moore CB, James IR & McKinnon EJ. Contribution of nucleoside analogue reverse transcriptase inhibitors to subcutaneous fat wasting in patients with HIV infection. *AIDS* 2000; 14:1309–1316.

5. Saint-Marc T, Partisani M, Poizot-Martin I, Rouviere O, Bruno F, Avellaneda R, Lang JM, Gastaut JA & Touraine JL. Fat distribution evaluated by computed tomography and metabolic abnormalities in patients undergoing antiretroviral therapy: preliminary results of the LIPOCO study. *AIDS* 2000; **14**:37–49.
6. Joly V, Flandre P, Meiffredy V, Leturque N, Harel M, Aboulker JP & Yeni P. Increased risk of lipodystrophy under stavudine in HIV-1-infected patients: results of a substudy from a comparative trial. *AIDS* 2002; **16**:2447–2454.
7. Law M, Emery S, French M, Carr A, Chuah J & Cooper D. Lipodystrophy and metabolic abnormalities in a cross-sectional study of participants in randomized controlled studies of combination antiretroviral therapy. *2nd International Workshop on Adverse Drug Reactions & Lipodystrophy*. September 13–15 2000. Toronto, Canada. Abstract O28.
8. Chene G, Angelini E, Cotte L, Lang JM, Morlat P, Rancinan C, May T, Journot V, Raffi F, Jarrousse B, Grappin M, Lepeu G & Molina JM. Role of long-term nucleoside-analogue therapy in lipodystrophy and metabolic disorders in human immunodeficiency virus-infected patients. *Clinical Infectious Diseases* 2002; **34**:649–657.
9. Dube MP, Zackin R, Tebas P *et al.* Prospective study of regional body composition in antiretroviral-naïve subjects randomized to receive zidovudine+lamivudine or didanosine+stavudine combined with nelfinavir, efavirenz, or both: A5005s, a substudy of ACTG 384. *4th International Workshop on Adverse Drug Reactions & Lipodystrophy*. September 22–25 2002, San Diego, Calif., USA. Abstract 27.
10. Saint-Marc T, Partisani M, Poizot-Martin I, Bruno F, Rouviere O, Lang JM, Gastaut JA & Touraine JL. A syndrome of peripheral fat wasting (lipodystrophy) in patients receiving long-term nucleoside analogue therapy. *AIDS* 1999; **13**:1659–1667.
11. Brinkman K, Smeitink JA, Romijn JA & Reiss P. Mitochondrial toxicity induced by nucleoside-analogue reverse-transcriptase inhibitors is a key factor in the pathogenesis of antiretroviral-therapy-related lipodystrophy. *Lancet* 1999; **354**:1112–1115.
12. Johnson AA, Ray AS, Hanes J, Suo Z, Colacino JM, Anderson KS & Johnson KA. Toxicity of antiviral nucleoside analogs and the human mitochondrial DNA polymerase. *Journal of Biological Chemistry* 2001; **276**:40847–40857.
13. Martin JL, Brown CE, Matthews-Davis N & Reardon JE. Effects of antiviral nucleoside analogs on human DNA polymerases and mitochondrial DNA synthesis. *Antimicrobial Agents & Chemotherapy* 1994; **38**:2743–2749.
14. Hammond EL, Sayer D, Nolan D, Walker UA, Ronde A, Montaner JS, Cote HC, Gahan ME, Cherry CL, Wesselingh SL, Reiss P & Mallal S. Assessment of precision and concordance of quantitative mitochondrial DNA assays: a collaborative international quality assurance study. *Journal of Clinical Virology* 2003; **27**:97–110.
15. Kingsley L, Smit E, Riddler S *et al.* Prevalence of lipodystrophy and metabolic abnormalities in the multicentre AIDS cohort study (MACS). *8th Conference on Retroviruses & Opportunistic Infections*. February 4–8 2001. Chicago, Ill., USA. Abstract 538.
16. Carr A, Workman C, Smith DE, Hoy J, Hudson J, Doong N, Martin A, Amin J, Freund J, Law M & Cooper DA; Mitochondrial Toxicity (MITOX) Study Group. Abacavir substitution for nucleoside analogs in patients with HIV lipodystrophy: a randomized trial. *Journal of the American Medical Association* 2002; **288**:207–215.
17. Dreschler H & Powderly WG. Switching effective antiretroviral therapy: a review. *Clinical Infectious Diseases* 2002; **35**:1219–1230.
18. Cherry C, Nolan D, James I *et al.* Longitudinal associations between antiretroviral treatments and quantification of tissue mitochondrial DNA from ambulatory subjects with HIV infection. *10th Conference on Retroviruses & Opportunistic Infections*. February 10–14 2003, Boston, Mass., USA. Abstract 133.
19. Nolan D, Hammond E, Martin A, Taylor L, Herrmann S, McKinnon E, Metcalf C, Latham B & Mallal S. Mitochondrial DNA depletion and morphologic changes in adipocytes associated with nucleoside reverse transcriptase inhibitor therapy. *AIDS* 2003; **17**:1329–1338.
20. Lloreta J, Domingo P, Pujol RM, Arroyo JA, Baixeras N, Matias-Guiu X, Gilaberte M, Sambeat MA & Serrano S. Ultrastructural features of highly active antiretroviral therapy-associated partial lipodystrophy. *Virchows Archives* 2002; **441**:599–604.
21. Walker UA, Bickel M, Lutke Volksbeck SI, Ketelsen UP, Schofer H, Setzer B, Venhoff N, Rickerts V & Staszewski S. Evidence of nucleoside analogue reverse transcriptase inhibitor-associated genetic and structural defects of mitochondria in adipose tissue of HIV-infected patients. *Journal of Acquired Immune Deficiency Syndromes* 2002; **29**:117–121.
22. Thompson K, McComsey G, Paulsen D *et al.* Improvements in body fat and mitochondrial DNA levels are accompanied by decreased adipose tissue apoptosis after replacement of stavudine therapy with either abacavir or stavudine. *10th Conference on Retroviruses & Opportunistic Infections*. February 10–14 2003, Boston, Mass., USA. Abstract 728.
23. Domingo P, Matias-Guiu X, Pujol RM, Domingo JC, Arroyo JA, Sambeat MA & Vazquez G. Switching to nevirapine decreases insulin levels but does not improve subcutaneous adipocyte apoptosis in patients with highly active antiretroviral therapy-associated lipodystrophy. *Journal of Infectious Diseases* 2001; **184**:1197–1201.
24. Behrens GM, Boerner AR, Weber K, van den Hoff J, Ockenga J, Brabant G & Schmidt RE. Impaired glucose phosphorylation and transport in skeletal muscle cause insulin resistance in HIV-1-infected patients with lipodystrophy. *Journal of Clinical Investigation* 2002; **110**:1319–1327.
25. Bastard JP, Caron M, Vidal H, Jan V, Auclair M, Vigouroux C, Luboinski J, Laville M, Maachi M, Girard PM, Rozenbaum W, Levan P & Capeau J. Association between altered expression of adipogenic factor SREBP1 in lipodystrophic adipose tissue from HIV-1-infected patients and abnormal adipocyte differentiation and insulin resistance. *Lancet* 2002; **359**:1026–1031.
26. Noor MA, Seneviratne T, Aweeka FT, Lo JC, Schwarz JM, Mulligan K, Schambelan M & Grunfeld C. Indinavir acutely inhibits insulin-stimulated glucose disposal in humans: a randomized, placebo-controlled study. *AIDS* 2002; **16**:F1–F8.
27. Gan SK, Samaras K, Thompson CH, Kraegen EW, Carr A, Cooper DA & Chisholm DJ. Altered myocellular and abdominal fat partitioning predict disturbance in insulin action in HIV protease inhibitor-related lipodystrophy. *Diabetes* 2002; **51**:3163–3169.
28. Sekhar RV, Jahoor F, White AC, Pownall HJ, Visnegarwala F, Rodriguez-Barradas MC, Sharma M, Reeds PJ & Balasubramanyam A. Metabolic basis of HIV-lipodystrophy syndrome. *American Journal of Physiology, Endocrinology & Metabolism* 2002; **283**:E332–E337.
29. Woerle HJ, Mariuz PR, Meyer C, Reichman RC, Popa EM, Dostou JM, Welle SL & Gerich JE. Mechanisms for the deterioration in glucose tolerance associated with HIV protease inhibitor regimens. *Diabetes* 2003; **52**:918–925.
30. Ford ES, Giles WH & Dietz WH. Prevalence of the metabolic syndrome among US adults: findings from the third National Health and Nutrition Examination Survey. *Journal of the American Medical Association* 2002; **287**:356–359.